Joint Detection for Generalized Optical MIMO: A Deep Learning Approach

Xin Zhong[1], Chen Chen[1,*], Lin Zeng[1], Ruochen Zhang[1], Yuru Tang[1], Yungui Nie[1], and Min Liu[1]
[1]School of Microelectronics and Communication Engineering, Chongqing University, China
[*]c.chen@cqu.edu.cn

2021 IEEE 16th Conference on Industrial Electronics and Applications (ICIEA) | 978-1-6654-2248-2/21/$31.00 ©2021 IEEE | DOI: 10.1109/ICIEA51954.2021.9516406

***Abstract*—In this paper, we investigate the performance of generalized optical multiple-input multiple-output (MIMO) systems using a deep learning-enabled joint detection scheme. In the generalized optical MIMO system applying both generalized spatial modulation (GSM) and generalized spatial multiplexing (GSMP), a fully connected deep neural network (DNN) is employed for the joint detection of spatial and constellation information. To efficiently train the DDN detector, the received signal after zero-forcing (ZF) equalization is taken as the input while the corresponding transmitted binary bits are used as the output. Our simulation shows that, in a 4×4 generalized optical MIMO system with two activated light-emitting diode (LED) transmitters, the ZF-DNN detector can achieve comparable bit error rate (BER) performance as the high-complexity joint maximum-likelihood (ML) detector in the high signal-to-noise ratio (SNR) region for both GSM and GSMP. Moreover, the ZF-DNN detector achieves substantially improved BER performance than the conventional ZF-based maximum-likelihood (ML) detector. Due to the ability to eliminate error propagation, the performance gain of GSMP over GSM is greatly improved by using the ZF-DNN detector in comparison to the ZF-ML detector.**

***Index Terms*—Visible light communication, generalized optical multiple-input multiple-output, deep learning.**

I. Introduction

Recently, due to the exhaustion of the radio frequency (RF) spectrum resources, optical wireless communication (OWC) using infrared, visible light or ultra-violet light-emitting diodes (LEDs) has been considered as a promising candidate to satisfy the ever-increasing data demand, especially in indoor environments [1]–[3]. Among them, visible light communication (VLC) using white LEDs has become a research hot spot, because LEDs have many advantages such as high energy efficiency, long lifetime, low cost and small size [4]. Nevertheless, commercial off-the-shelf white LEDs usually have a very small electrical bandwidth, which limits the achievable capacity of VLC systems. Multiple-input multiple-output (MIMO) transmission is one of the most efficient techniques to improve the capacity of VLC systems due to its ability to provide substantial diversity or multiplexing gain [5]–[8]. Among them, spatial multiplexing (SMP) and spatial modulation (SM) are two main MIMO techniques applied in VLC systems. SMP can achieve full multiplexing gain and relative high spectral efficiency, but it suffers from severe inter-channel interference [9]. SM activates one LED to transmit signal at each time slot and additional bits can be transmitted by selecting the index of the activated LED [10]. Nevertheless, it is challenging for SM to achieve high spectral efficiency. In recent years, generalized optical MIMO techniques, including generalized spatial modulation (GSM) and generalized spatial multiplexing (GSMP), have been further proposed to boost the achievable capacity of MIMO VLC systems [11]. In GSM, more than one LED can be selected to transmit the same signal, resulting in high diversity gain. GSMP can be seen as the combination of digital modulation and SMP, which activates a subset of LEDs to transmit different signals.

In generalized optical MIMO systems, the joint maximum-likelihood (ML) detector can achieve the optimal bit error rate (BER) performance, but with very high computational complexity [12]. The combination of zero-forcing (ZF) equalization and ML detection of spatial symbols can be a low-complexity detection scheme for generalized optical MIMO systems [11]. However, ZF equalization inevitably amplifies the noise, leading to significant performance loss. Therefore, traditional detection scheme usually cannot achieve optimal BER performance with low complexity in generalized optical MIMO systems.

Nowadays, deep learning techniques have been widely used in many areas, including object recognition, image processing and wireless communication [13]. Moreover, deep learning techniques have also been considered in VLC systems for the design binary signaling [14], the mitigation of both linear and nonlinear impairments [15], the energy-efficient resource management [16], the detection of OFDM signals [17], and so on. Specifically, a deep learning-based detection scheme has been proposed for MIMO-VLC systems using GSM in [18]. Nevertheless, the performance of deep learning-based detection in generalized optical MIMO systems has not yet been fully investigated in the literature.

In this paper, we investigate the performance of the deep learning-enabled joint detection scheme in generalized optical MIMO systems, including GSM and GSMP. The deep learning-enabled joint detection is realized by a fully connected deep neural network (DNN), where the DNN is trained by taking the received signal after ZF equalization as the input and the corresponding transmitted binary bits as the output. Our simulation results show that the ZF-DNN detector can achieve near-optimal BER performance as the high-complexity joint ML detector, which greatly outperforms the ZF-based ML detector. It is also shown that the ZF-DNN detector can

This work was supported by the National Natural Science Foundation of China under Grant 61901065.

improve the performance gain of GSMP over GSM when compared with the ZF-based ML detector.

II. System Model

A. MIMO-VLC Channel Model

We first describe the channel model of the MIMO-VLC system equipped with N_t LED transmitters and N_r photodiode (PD) receivers. Let $\mathbf{x} = [x_1, x_2, \cdots, x_{N_t}]^T$ be the transmitted signal vector, $\mathbf{H}$ represent the $N_r \times N_t$ MIMO channel matrix and $\mathbf{n} = [n_1, n_2, \cdots, n_{N_r}]^T$ denote the additive noise vector. The received signal vector $\mathbf{y} = [y_1, y_2, \cdots, y_{N_r}]^T$ can be given by :

$$\mathbf{y} = \mathbf{H}\mathbf{x} + \mathbf{n}, \tag{1}$$

where the channel matrix of the $N_r \times N_t$ MIMO-VLC system can be expressed as follows:

$$\mathbf{H} = \begin{bmatrix} h_{11} & \cdots & h_{1N_t} \\ \vdots & \ddots & \vdots \\ h_{N_r1} & \cdots & h_{N_rN_t} \end{bmatrix}, \tag{2}$$

where h_{rt} ($r = 1, 2, \cdots, N_r; t = 1, 2, \cdots, N_t$) is the channel gain between the r-th PD and the t-th LED. Assuming the LED follows a Lambertian radiation pattern and only the line-of-sight (LOS) transmission is considered [5], we have:

$$h_{rt} = \begin{cases} \frac{(l+1)\rho A}{2\pi d_{rt}^2}\cos^m(\varphi_{rt})T_s G\cos(\theta_{rt}) & 0 \le \theta_{rt} \le \Phi \\ 0 & \theta_{rt} > \Phi \end{cases} \tag{3}$$

where $l = -\ln 2/\ln(\cos(\Psi))$ is the Lambertian emission order and Ψ denotes the semi-angle at half power of the LED; ρ and A are the responsivity and the active area of the PD, respectively; T_s is the gain of optical filter; $G = \frac{n^2}{\sin^2\Phi}$ is the gain of optical lens, where n and Φ are the refractive index and the half-angle field-of-view (FOV) of the optical lens, respectively; the distance between the r-th PD and the t-th LED, the emission angle and the incident angle are denoted as d_{rt}, φ_{rt} and θ_{rt}, respectively.

Moreover, the additive noise n_r ($r = 1, 2, \cdots, N_r$) in the MIMO-VLC system usually consists of both shot and thermal noises, which can be reasonably modeled as a real-valued zero-mean additive white Gaussian noise (AWGN) with power $P_n = N_0 B$, where N_0 and B denote the noise power spectral density (PSD) and the modulation bandwidth, respectively.

B. GSM and GSMP Using PAM

In this subsection, we describe the principle of two generalized optical MIMO techniques, including GSM and GSMP, using M-ary pulse amplitude modulation (PAM) modulation.

Fig. 1(a) illustrates the schematic diagram of GSM using M-PAM modulation with N_t = 4 and N_a = 2, where N_a is the number of activated LEDs. As we can see, the input bits are first divided into two parts, i.e., the constellation part and the spatial part. Then, the constellation part is modulated into PAM symbols. For M-ary PAM modulation, the intensity levels of the PAM symbols are given by

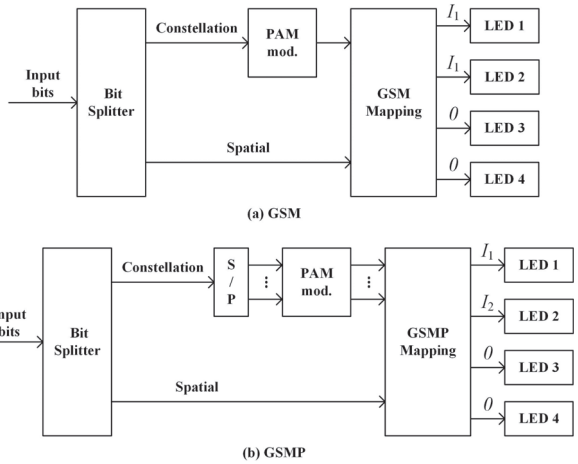

Fig. 1. Schematic diagram of (a) GSM and (b) GSMP using M-PAM modulation with N_t = 4 and N_a = 2.

$$I_m = \frac{2mI}{M+1}, \quad m = 1, \cdots, M, \tag{4}$$

where I denotes the average optical power emitted. Finally, these PAM symbols are assigned to the specified LEDs according to the GSM mapping rule. Hence, the spectral efficiency (bits/s/Hz) of GSM using M-PAM modulation can be calculated by:

$$R_{\text{GSM}} = \log_2 M + \left\lfloor \log_2(C_{N_t}^{N_a}) \right\rfloor, \tag{5}$$

where $\lfloor \cdot \rfloor$ denotes the floor function and $C_{N_t}^{N_a}$ represents the corresponding binomial coefficient.

The schematic diagram of GSMP using M-PAM modulation with N_t = 4, N_a = 2 is depicted in Fig. 1(b). Similar to GSM, the input bits are first divided into two parts, but the serial constellation bit stream for constellation mapping is further converted into N_a parallel bit streams via serial-to-parallel (S/P) conversion. Then the parallel bit streams are modulated into N_a parallel PAM symbols. Finally, the resultant PAM symbols are assigned to the specified LEDs according to the GSMP mapping rule. The main difference between GSM and GSMP is that GSMP requires two different signals at each time slot for N_a = 2, whereas GSM requires only two copies of the same signal. Therefore, the spectral efficiency (bits/s/Hz) of GSMP using M-PAM modulation is given by:

$$R_{\text{GSMP}} = N_a \log_2 M + \left\lfloor \log_2(C_{N_t}^{N_a}) \right\rfloor. \tag{6}$$

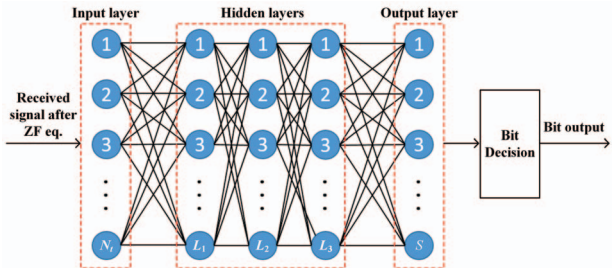

Fig. 2. Block diagram of the ZF-DNN detector for generalized optical MIMO.

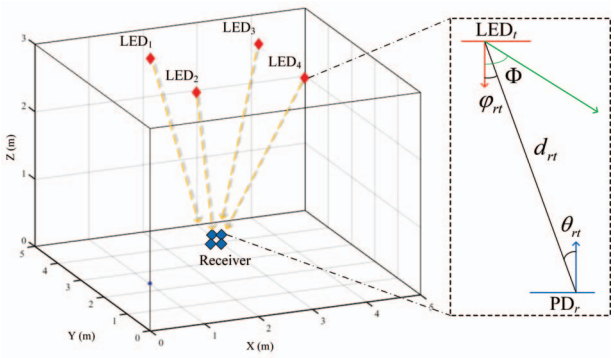

Fig. 3. Geometric setup of the 4 × 4 MIMO-VLC system.

C. Detection Schemes

1) Joint ML Detection: Under the assumption of perfect channel state information and ideal time synchronization, the joint ML detector is the optimal detector for MIMO-VLC systems employing GSM and GSMP with M-PAM modulation. The joint ML detector can jointly recover the transmitted constellation and spatial information, which is given by

$$(\hat{\mathbf{s}}, \hat{\mathbf{i}}) = \arg \min_{s \in \mathbb{S}, i \in \mathbb{I}} \|\mathbf{y} - \mathbf{H}\mathbf{x}\|^2, \tag{7}$$

where $\hat{\mathbf{s}}$ is the estimated transmitter combination with $\mathbb{S}$ being the set of all the considered transmitter combinations, $\hat{\mathbf{i}}$ is the estimated constellation symbol vector with $\mathbb{I}$ being the set of all possible N_a-dimensional constellation symbol vectors, and $\|\cdot\|$ denotes the Euclidean norm.

Although the joint ML detector can achieve optimal performance, it suffers from high computational complexity. Hence, it is usually not quite feasible to apply the joint ML detector in practical systems.

2) ZF-Based ML Detection: To avoid the high computational complexity of the joint ML detector, the low-complexity ZF-based ML detector can be adopted for MIMO-VLC systems employing GSM and GSMP [11]. During the ZF-based ML detection, ZF equalization is first executed and the obtained signal can be expressed by

$$\hat{\mathbf{x}} = \mathbf{H}^{\dagger}\mathbf{y} = \mathbf{x} + \mathbf{H}^{\dagger}\mathbf{n}, \tag{8}$$

where $\mathbf{H}^{\dagger}$ denotes the pseudo inverse of $\mathbf{H}$. After ZF equalization, the resultant signal is then utilized to perform ML detection so as to obtain the spatial symbols. Subsequently, using the obtained spatial information, the constellation symbols can be extracted for demodulation accordingly. For more details about the ZF-ML detector, please refer to [11].

By performing ZF equalization before the ML detection, the ZF-ML detector can significantly reduce the computational complexity when comparing with the joint ML detector, but it suffers from the adverse effect of significant noise amplification.

3) DNN-Based Joint Detection: To address the high complexity issue of the joint ML detector and the noise amplification issue of the ZF-ML detector, a deep learning-based joint detection scheme has been proposed for MIMO-VLC systems using GSM in [18].

TABLE I
SIMULATION PARAMETERS.

Parameters of GSMP/GSM	Value
Number of activated LED	2
Input nodes	4
Hidden layer	3
Output nodes	4
Hidden layer activation	ReLu
Output layer activation	Sigmoid
Loss function	MSE
Optimizer	Adam
Learning rate	0.001
Number of training set	100000
Number of validation set	50000
Epoch	50 / 40
Hidden nodes	32-16-16
Spectral efficiency	4bits/s/Hz
LED spacing	2 m
PD spacing	10 cm
Semi-angle at half power of LED	60°
Responsivity of the PD	1 A/W
Active area of PD	1 cm^2
Refractive index	1.5
Half-angle FOV of optical lens	72°
Noise PSD	$10^{-22} A^2$/Hz
Signal bandwidth	20 MHz

As illustrated in Fig. 2, the ZF-DNN detector consists of one input layer, three hidden layers, one output layer and a bit decision module. The received signal after ZF equalization is taken as the input of the ZF-DNN detector, and hence the input layer has totally N_t neurons accordingly. In the ZF-DNN detector, three fully connected hidden layers with L_1, L_2 and L_3 neurons in these layers respectively are considered, which are used to learn the statistical characteristics of both the input signal and the additive noise. The rectified linear unit (ReLU) function, i.e., $f_{\mathrm{ReLU}}(\alpha) = \max(0, \alpha)$, is adopted as the activation function of the hidden layers. The output layer of the ZF-DNN detector generates a fuzzy bit information, which adopts the Sigmoid function, i.e., $f_{\mathrm{Sigmoid}}(\alpha) = 1/(1 + \exp^{-\alpha})$, as the activation function so as to map the output into the range [0,1]. Since the ZF-DNN detector takes the transmitted binary bits corresponding to a transmitted signal vector as the output, the number of neurons in the output layer is equal to the number of the output bits. Therefore, the input-output

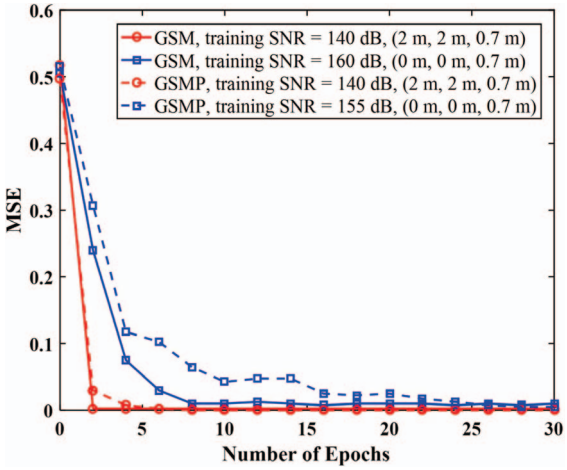

Fig. 4. MES loss of the ZF-DNN detector for GSM and GSMP with two receiver locations.

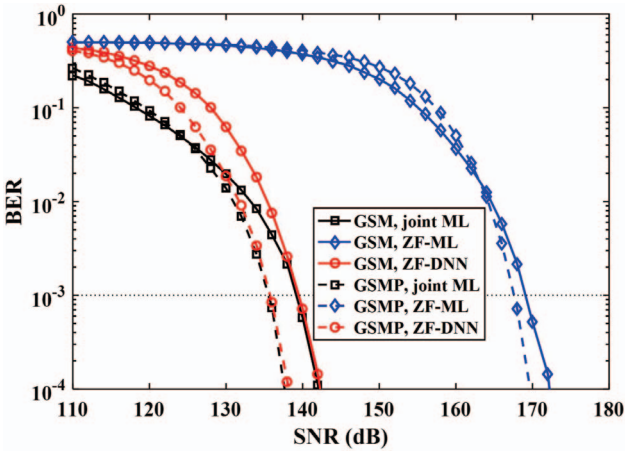

Fig. 5. BER vs. transmit SNR for GSM and GSMP in the 4×4 MIMO-VLC system with different detection schemes. The receiver position is (2 m, 2 m, 0.7 m) and the spectral efficiency is 4 bits/s/Hz .

relationship of the L^{th} layer of the DNN can be expressed by

$$\mathbf{L}^n = \begin{cases} f_{\mathrm{ReLU}}\left(\mathbf{W}_{n-1}\mathbf{L}^{n-1} + \mathbf{b}_{n-1}\right), & 2 \le n \le 4 \\ f_{\mathrm{Sigmoid}}\left(\mathbf{W}_{n-1}\mathbf{L}^{n-1} + \mathbf{b}_{n-1}\right), & n = 5 \end{cases} \tag{9}$$

where W_n and $\mathbf{b}_n$ represent the weight matrix and the bias vector, respectively. Finally, the bit decision module is utilized to determine the fuzzy output to be 0 or 1. Let $\mathbf{L^5} = [k_1, k_2, \ldots k_s]^T$ denote the output vector with s being the number of the neurons in the output layer, the estimated bits $\hat{B}_s$ can be obtained by

$$\hat{B}_s = \begin{cases} 0, & k_s < 0.5 \\ 1, & k_s \ge 0.5 \end{cases} \tag{10}$$

In the ZF-DNN detector, the mean-squared error (MSE) loss function is adopted to measure the difference between the estimated bits $\hat{B}_s$ and the transmitted bits B_s:

$$MSE = \frac{1}{s}\left\|\hat{B}_s - B_s\right\|^2. \tag{11}$$

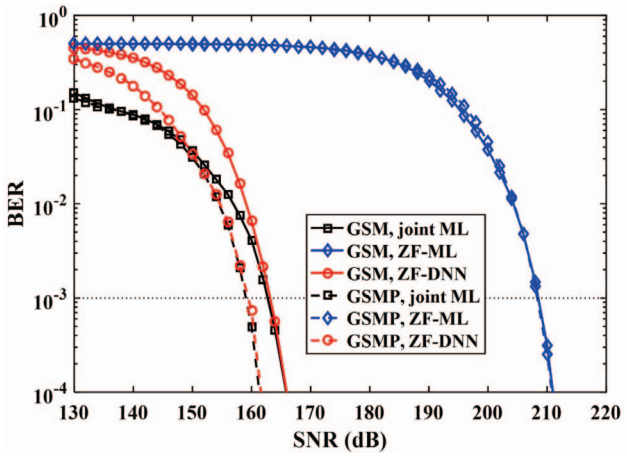

Fig. 6. BER vs. transmit SNR for GSM and GSMP in the 4×4 MIMO-VLC system with different detection schemes. The receiver position is (0 m, 0 m, 0.7m) and the spectral efficiency is 4 bits/s/Hz.

III. Simulation Results

In this section, computer simulations are performed to evaluate the performance of the ZF-DNN detector in generalized optical MIMO systems. We consider a 4 × 4 MIMO-VLC system configured in a typical room with a dimension of 5 m × 5 m × 3 m. Fig. 3 depicts the geometric setup of the 4 × 4 MIMO-VLC system, where the 2 × 2 LED array is placed at the center of the ceiling and the separation between two adjacent LEDs is 2 m. Two receiver positions, including (2 m, 2 m, 0.7m) and (0m, 0m, 0.7m), are considered for performance evaluation. Each receiver consists of a 2 × 2 PD array, where the separation between two adjacent PDs in the receiver is 10 cm. The detailed simulation parameters can be found in Table I. Note that the ZF-DNN detector is trained under the optimal signal-to-noise (SNR) condition for each receiver position. In addition, we use the Mini-Batch technique in training so as to accelerate the convergence speed and each mini-batch contains 100 transmitted symbol vectors. To ensure fairness, the same spectral efficiency of 4 bits/s/Hz is adopted for both GSM and GSMP. Moreover, for the purpose of performance comparison, the joint ML detector and the ZF-ML detector are also considered as the benchmark ones.

Fig. 4 shows the MSE loss versus the number of epochs of the ZF-DNN detector for GSM and GSMP with two receiver locations. As we can see, the MSE loss decreases rapidly with the increase of the number of epochs for each case. Moreover, the optimal training SNRs for GSM at (2 m, 2 m, 0.7 m) and (0 m, 0 m, 0.7 m) are 140 and 160 dB, respectively, and the optimal training SNRs for GSMP at (2 m, 2 m, 0.7 m) and (0 m, 0 m, 0.7 m) are 140 and 155 dB, respectively.

Figs. 5 and 6 compare the BER performance of different detection schemes for GSM and GSMP at the receiver position of (2 m, 2 m, 0.7 m) and (0 m, 0 m, 0.7 m), respectively. At the

receiver position of (2 m, 2 m, 0.7 m), as shown in Fig. 5, the required SNR for GSM with the joint ML detector to achieve BER = 10^{-3} is about 139 dB. When the ZF-ML detector is applied for GSM, the required SNR to reach BER = 10^{-3} becomes about 169 dB, indicating an SNR reduction of as high as 30 dB due to severe noise amplification during the ZF-ML detection. Moreover, when using the joint ML detector, GSMP outperforms GSM by an SNR gain of 3.5 dB. However, the SNR gain is reduced to only 1.5 dB when the ZF-ML detector is used, which is mainly due to the error propagation effect during the ZF-ML detection. It can be further seen from Fig. 5 that the ZF-DNN detector can achieve optimal BER performance as the joint ML detector at large SNR regions for both GSM and GSMP, and the 3.5-dB SNR can be maintained by utilizing the ZF-DNN detector in comparison to the ZF-ML detector. When the receiver is moved to position (0 m, 0 m, 0.7 m), the performance gain of GSMP over GSM becomes negligible when using the ZF-ML detector. However, an SNR gain of 3.7 dB can be obtained by employing the joint ML detector or the ZF-DNN detector. These results suggest that the ZF-DNN detector has the ability to mitigate both noise amplification and error propagation suffered by the ZF-ML detector, especially when the receiver is more close to the corner of the room.

IV. Conclusion

In this paper, we have investigated the performance of the ZF-DNN detector in generalized optical MIMO systems including GSM and GSMP. Our simulation results show that, in an indoor 4×4 MIMO-VLC system with $N_a = 2$ and a spectral efficiency of 4 bits/s/Hz, the ZF-DNN detector can achieve optimal BER performance as the joint ML detector. Moreover, it is also shown that the ZF-DNN detector can not only eliminate the adverse noise amplification effect but also mitigate the adverse error propagation effect suffered by the ZF-ML detector. Therefore, the ZF-DNN detector can be very promising for high-speed MIMO-VLC systems.

References

[1] Z. Ghassemlooy, S. Arnon, M. Uysal, Z. Xu, and J. Cheng, "Emerging optical wireless communications-advances and challenges," *IEEE J. Sel. Areas Commun.*, vol. 33, no. 9, pp. 1738–1749, Sep. 2015.

[2] T. Cogalan and H. Haas, "Why would 5G need optical wireless communications?" in *Proc. IEEE Ann. Int. Symp. Pers., Indoor Mobile Radio Commun. (PIMRC)*, Oct. 2017, pp. 1–6.

[3] C. Chen, S. Fu, X. Jian, M. Liu, X. Deng, and Z. Ding, "NOMA for energy-efficient LiFi-enabled bidirectional IoT communication," *IEEE Trans. Commun.*, vol. 69, no. 3, pp. 1693–1706, Mar. 2021.

[4] T. Komine and M. Nakagawa, "Fundamental analysis for visible-light communication system using LED lights," *IEEE Trans. Consum. Electron.*, vol. 50, no. 1, pp. 100–107, Feb. 2004.

[5] L. Zeng, D. C. O'Brien, H. Le Minh, G. E. Faulkner, K. Lee, D. Jung, Y. Oh, and E. T. Won, "High data rate multiple input multiple output (MIMO) optical wireless communications using white LED lighting," *IEEE J. Sel. Areas Commun.*, vol. 27, no. 9, pp. 1654–1662, Dec. 2009.

[6] T. Fath and H. Haas, "Performance comparison of MIMO techniques for optical wireless communications in indoor environments," *IEEE Trans. Commun.*, vol. 61, no. 2, pp. 733–742, Feb. 2013.

[7] C. Chen, W.-D. Zhong, and D. Wu, "On the coverage of multiple-input multiple-output visible light communications [Invited]," *J. Opt. Commun. Netw.*, vol. 9, no. 9, pp. D31–D41, Sep. 2017.

[8] C. Chen, W.-D. Zhong, H. Yang, and P. Du, "On the performance of MIMO-NOMA-based visible light communication systems," *IEEE Photon. Technol. Lett.*, vol. 30, no. 4, pp. 307–310, Feb. 2018.

[9] C. Chen, H. Yang, P. Du, W.-D. Zhong, A. Alphones, Y. Yang, and X. Deng, "User-centric MIMO techniques for indoor visible light communication systems," *IEEE Syst. J.*, vol. 14, no. 3, pp. 3202–3213,, Sep. 2020.

[10] R. Mesleh, H. Elgala, and H. Haas, "Optical spatial modulation," *J. Opt. Commun. Netw.*, vol. 3, no. 3, pp. 234–244, Mar. 2011.

[11] C. Chen, X. Zhong, S. Fu, X. Jian, M. Liu, H. Yang, A. Alphones, and H. Y. Fu, "OFDM-based generalized optical MIMO," 2021. [Online]. Available: https://doi.org/10.36227/techrxiv.13270751.v1.

[12] T. Özbilgin and M. Koca, "Optical spatial modulation over atmospheric turbulence channels," *J. Lightw. Technol.*, vol. 33, no. 11, pp. 2313–2323, Jun. 2015.

[13] Y. LeCun, Y. Bengio, and G. Hinton, "Deep learning," *Nature*, vol. 521, no. 7553, pp. 436–444, May 2015.

[14] H. Lee, I. Lee, T. Q. Quek, and S. H. Lee, "Binary signaling design for visible light communication: A deep learning framework," *Opt. Exp.*, vol. 26, no. 14, pp. 18 131–18 142, Jul. 2018.

[15] X. Lu, C. Lu, W. Yu, L. Qiao, S. Liang, A. P. T. Lau, and N. Chi, "Memory-controlled deep LSTM neural network post-equalizer used in high-speed PAM VLC system," *Opt. Exp.*, vol. 27, no. 5, pp. 7822–7833, Mar. 2019.

[16] H. Yang, A. Alphones, W.-D. Zhong, C. Chen, and X. Xie, "Learning-based energy-efficient resource management by heterogeneous RF/VLC for ultra-reliable low-latency industrial IoT networks," *IEEE Trans. Ind. Informat.*, vol. 16, no. 8, pp. 5565–5576, Aug. 2019.

[17] N. A. Amran, M. D. Soltani, M. Yaghoobi, and M. Safari, "Deep Learning Based Signal Detection for OFDM VLC Systems," in *Proc. IEEE Int. Conf. Commun. Workshops (ICC Workshops)*, Jun. 2020, pp. 1–6.

[18] T. Wang, F. Yang, and J. Song, "Deep learning-based detection scheme for visible light communication with generalized spatial modulation," *Opt. Exp.*, vol. 28, no. 20, pp. 28 906–28 915, Sep. 2020.